International Food Research Journal 32(2): 552 - 564 (April 2025)
Journal homepage: *http://www.ifrj.upm.edu.my*

Optimisation of ultrasonic-assisted enzyme extraction to analyse total flavonoids and antioxidant activity of purple potato using response surface and artificial neural networks model

[1]Cao, F., [1]Chen, X., [1]Huang, A., [1]Hu, J. and [2]*Yang, D.

[1]*Department of Food and Safety, Bengbu Medical University, Bengbu, 233000 Anhui, China*
[2]*Department of Computer and Science, Bengbu Medical University, Bengbu, 233000 Anhui, China*

Article history

Received:
27 August 2024
Received in revised form:
25 March 2025
Accepted:
9 April 2025

Keywords

antioxidant application,
free radical scavenging activity,
predictive mode,
process parameter optimisation,
ultrasonic-enzymatic synergy

Abstract

The present work utilised purple potatoes as the raw material to perform response surface methodology (RSM) and an artificial neural network (ANN) model. The objectives of the present work were to enhance the efficiency of ultrasound-assisted enzymatic extraction of total flavonoids from purple potatoes, and evaluate their antioxidant activity. The results demonstrated that the ANN model achieved a higher predictive accuracy, with a correlation coefficient of 0.99553 than the RSM model (R^2 = 0.9919). The optimal extraction process conditions were the addition of 51.34 U/mL enzyme, extraction duration of 36.21 min, and extraction temperature of 53.12°C. The total flavonoid yield was 9.81 mg/g under these conditions, suggesting higher prediction ability of ANN. The scavenging rates of OH· and DPPH·(2,2-diphenyl-1-picrylhydrazyl) were 81.6 and 61.8%, respectively, for the purple potato extract concentration of 0.24 mg/mL. The present work proposes a novel approach integrating ANN with ultrasonic-assisted enzymatic extraction to predict and optimise flavonoid yields, demonstrating superior accuracy over traditional methods. The findings advance the extraction of bioactive compounds, and highlight ANN's potential for modelling complex non-linear relationships in food science.

DOI
https://doi.org/10.47836/ifrj.32.2.18

Introduction

Purple potatoes (*Solanum tuberosum* L.) are tubers with purplish-red roots. They are also known as as purple sweet potatoes or black potatoes. Originally, they were primarily cultivated in New Zealand, South Korea, and Japan. Presently, however, they are also grown extensively in China (Steed and Truong, 2008). Purple potato is ranked as the seventh largest crop globally after rice, wheat, maize, potato, sugarcane, and cassava. However, their nutritional and health potential has neither been properly explored nor utilised (Esatbeyoglu *et al*., 2017). Purple potatoes are rich in carbohydrates, dietary fibres, carotenes, minerals, and a diverse range of bioactive compounds. Flavonoids are critical bioactive constituents of plant secondary metabolites, and found abundantly in purple potatoes (Cai *et al*., 2016; Huang *et al*., 2019; Wang *et al*., 2022). They may be classified into many types such as flavonoids, flavonols, flavanones, isoflavones, and anthocyanins (Panche *et al*., 2016). Notably, flavonoids exhibit a multitude of functional attributes such as anti-inflammatory, antiviral, hypoglycaemic, antioxidant, and liver-protective properties (Corcoran *et al*., 2012; Samsonowicz *et al*., 2019; Luo *et al*., 2021; Badshah *et al*., 2021).

Traditional methods for extracting phytochemicals, such as solvent extraction, are widely used due to their simplicity and cost-effectiveness. However, they suffer from low selectivity, environmental and health risks, and potential degradation of heat-sensitive compounds (Chen *et al*., 2022). Enzyme-assisted extraction improves selectivity by targeting specific cell wall components, but faces challenges such as high costs and sensitivity to operational conditions (Amiri-Rigi *et al*., 2016). Ultrasonic-assisted enzymatic extraction (UAEE) was selected as the primary method in the present work due to its synergistic advantages in enhancing flavonoid yield and efficiency (Wu *et al*., 2014; Nag and Sit, 2018). Ultrasonication generates

*Corresponding author.
Email: zyzprime@gmail.com

cavitation bubbles that disrupt plant cell walls, facilitating the release of intracellular compounds and enzymatic hydrolysis by cellulase, pectinase, and hemicellulose, and specifically targets the polysaccharides present in the cell wall, further improving extraction efficiency (Ahmad-Qasem *et al*., 2013; Singla and Sit, 2021). This combined approach is particularly suitable for purple potatoes, because their dense cellular structure and high starch content pose challenges when conventional extraction methods are used. Moreover, UAEE operates at lower temperatures than the thermal methods, preserving the stability and bioactivity of heat-sensitive flavonoids (Hou *et al*., 2019). Besides, aspects of scalability, cost-effectiveness, and environmental sustainability align with the growing demand for green extraction technologies in the food and pharmaceutical industries.

Response surface methodology (RSM) is a valuable technique for mathematical modelling and statistical analysis. It is well known for its simplicity, speed, and reliability. RSM is commonly employed to optimise the extraction of bioactive compounds such as flavonoids, polyphenols, and polysaccharides. It is extensively used in fields such as food engineering, bioprocessing, and pharmaceuticals (Liu *et al*., 2017; Riciputi *et al*., 2018). Artificial neural networks (ANN) are computational modelling methods that imitate biological neural networks to process information in a distributed and parallel manner. It can tolerate errors, learn on its own, and adapt and approximate data accurately. ANN are widely used to extract and parametrise bioactive substances (Onukwuli *et al*., 2021; Wu *et al*., 2024). Moreover, ANN exhibit greater adaptability than RSM, which enables them to effectively handle complex non-linear interactions, and construct models by learning from experimental data. Ciric *et al.* (2020) successfully determined the optimal process conditions for extracting polyphenols from garlic using UAEE, and employing both RSM and ANN. Their findings demonstrated a strong correlation between the predicted values from the ANN model and the actual total phenol and total flavonoid contents, with coefficients of correlation (R) of 0.9998, 0.9733, and 0.9821 for the training, validation, and testing phases, respectively. These results indicated that the ANN model outperformed the RSM model in terms of predictive accuracy and efficiency.

Apart from these sporadic studies, there is limited research utilising ANN in combination with UAEE of bioactive compounds from purple potatoes. To address this gap, we employed UAEE to extract total flavonoids from purple potatoes. The RSM and ANN integration optimised the extraction conditions for total flavonoids, demonstrating a robust methodological framework that can be adapted by future studies to extract bioactive compounds. Furthermore, an analytical assessment of the antioxidant activity of the flavonoids was conducted to establish a solid research foundation for the extraction of active substances from plants.

Materials and methods

Chemicals

DPPH (98.5% purity), methanol, and phosphate (HPLC ≥ 99.9%) were obtained from Macklin Co. Ltd. (Shanghai, China); rutin, quercetin, and kaempferol (HPLC ≥ 98%) were obtained from Shanghai Yuanye Bio-Technology Co., Ltd. (Shanghai, China); and hemicellulase (≥ 200 U/mg) was obtained from Aladdin Reagent Co., Ltd. (Shanghai, China). The remaining chemicals (analytical grade) were obtained from Sinopharm Chemical Reagent (Shanghai, China).

Sample preparation

Purple-flesh potatoes, each weighing approximately 90 g with a uniform shape (length: 9 - 11 cm; diameter: 4 - 5 cm), and harvested in October 2022, were sourced from a local market in Bengbu, China.

Fresh purple potatoes were thoroughly cleaned and cut into 5 mm slices, dried at a constant temperature of 40°C in an electric thermostatic drying oven (Shanghai Yuejin Medical Equipment Co., Ltd., China), crushed and ground, passed through a 40-mesh sieve, sealed, and stored under a shady shade.

Ultrasound-assisted enzymatic extraction

Extraction of total flavonoids

Purple potatoes were placed in a brown reagent bottle soaked in acidified ethanol, homogeneously mixed, rehydrated for 30 min, and extracted in a PS-20A ultrasonic bath (Changzhou Henglong Instrument Co., Ltd., China). The mixture was then centrifuged at 5,000 rpm for 10 min in a JW-3021H centrifuge (Anhui Jiawen Instrument

Co., Ltd., China). The extract was concentrated to remove ethanol, and adjusted to a fixed volume. Finally, the purple potato extract solution was stored at 4°C for 12 h. Following this, the concentrated extract was frozen and dried to produce purple potato extract.

Effect of individual factors on TFY

The method reported by Cai *et al*. (2016) was followed with slight modifications. Briefly, 0.5 g of purple potato powder was placed in a brown glass tube, and mixed with acidified ethanol (0.1% of HCL and C_2H_5OH in a ratio of 4:6) as the extractor. The fixed material ratio was 1:20, and the ultrasound power was 120 W. Next, the effects of hemicellulase addition (30, 40, 50, 60, and 80 μmL); extraction duration (20, 25, 30, 35, and 40 min); and temperature (40, 45, 50, 60, and 65°C) on the total flavonoid yields (TFY) of purple potatoes were examined.

Response Surface Methodology

Based on a single-factor test, RSM was used to examine how total flavonoid extraction was affected when purple potatoes were simultaneously treated with ultrasound and enzymes. The Box-Behnken responsive surface test design was used with three variables (enzyme addition, A; extraction time, B; and temperature, C) at three levels (-1, 0, and 1) to evaluate the effect of the two interaction terms on TFY.

Artificial Neural Networks

The ANN, a computational model inspired by biological neural networks, comprises interconnected neurons that process and analyse input data using adjustable synaptic weights and thresholds to generate the corresponding outputs. The literature corroborates the superior predictive capabilities of ANN over the RSM (Wu *et al*., 2024). Therefore, based on the RSM experimental results, the neural network fitting toolbox in MATLAB was employed to develop a predictive model for the experimental data generated from purple potatoes. This model established a non-linear relationship between the three input variables (independent variables) and the response (target output). The architecture of the network, comprising an input layer (variables A, B, and C) and an output layer, was determined using a Box-Behnken design (BBD). To mitigate the overfitting risks associated with excessive hidden layers, a single hidden layer was implemented, and the Levenberg-Marquardt backpropagation algorithm was utilised for network optimisation. The structural configuration of the model was as follows.

(1) Input layer design

Based on the results of the single factor experiments, enzyme addition, temperature, and extraction duration were installed as input layer nodes of the network model, and used as naturalisation treatments in Eq. 1:

$$X'_{ip} = \frac{X_{ip} - min(X_{ip})}{max(X_{ip}) - min(X_{ip})} \quad \text{(Eq. 1)}$$

where, X_{ip}= primary training sample input data, $\min(X_{ip})$ and $\max(X_{ip})$= minimum and maximum values in the input training sample data, respectively, and X'_{ip}= result of the naturalisation. All the datasets were mapped in between $[0,1]$. The sample datasets obtained were divided into three groups: 70% for training, 15% for testing, and 15% for validation. At the same time, the input of the layers in the network was updated in Eqs. 2 and 3:

$$x_j = \sum_i w_{ij} x'_{ip} \quad \text{(Eq. 2)}$$

$$y_n(k) = \sum_j w_{jk} x'_j \quad \text{(Eq. 3)}$$

In this case, the connection values between the input and intermediate layers, and between the intermediate and output layers, were defined as w_{ij} and w_{jk}, respectively.

(2) Intermediate layer design

The primary function of the intermediate layer in an ANN is to extract and modify the characteristics of input sample data to facilitate enhanced learning and prediction capabilities in the output layer. Generally, the larger the number of layers in the intermediate layer and the more neuronal nodes, the stronger the network's expression capacity; however, it also increases the network training duration and computational costs. Considering the stability and saturation of the sample dataset in the intermediate layer processing, to improve the model's computational efficiency and to avoid over-adaptation during sample dataset training, the intermediate layer had one layer and the activation function for each neuronal node was selected as

Rectified Linear Unit (Relu). When determining the number of intermediate-layer neurons N_m, Eq. 4 was used:

$$N_m = \frac{\alpha * \sqrt{N_i + N_o}}{N_s} + \beta \quad \text{(Eq. 4)}$$

where, N_i and N_o = numbers of neurons in the input and output layers, respectively, and N_s = number of samples in the training set $\alpha,\ \beta \in [0,1]$. To minimise the network error and model training time, the relevant coefficient adjustment was performed using the test error method to obtain the optimal combination of the implicit layer and passing function (minimum error condition), and the adjusted parameter when the number of neurons $N_m = 9$ and the above conditions were met (Hornik *et al*., 1989; Said *et al*., 2020).

(3) Particle swarm optimisation (PSO) artificial neural network algorithm

Owing to the limited linear generalisation capacity and slow convergence rate of traditional ANN, there is a high likelihood of encountering local minima, and increased mistakes during the computation process. The particle swarm optimisation algorithm is used to optimise the weights between the intermediate and output layer, and differs from other optimisation algorithms (*e.g*., genetic and gradient descent algorithm). It extracts the behavioural characteristics of the acquired sample individuals, and interacts with the information of the individual and the global extremum in the cooperative game, which is suitable for dealing with the complex interaction between multiple variables such as enzyme addition, time, and temperature in the UAEE. In addition, the network weights are dynamically adjusted based on historical empirical data, effectively avoiding the trap of local minima to improve the prediction accuracy and stability of the ANN, and eventually realise the search for the optimal weights of individuals in the solvable space. In the *D*-dimensional search space, there are *n* sample datapoints composed of particle populations as $X(X_1, X_2, \cdots, X_n)$, where the position information of the *i*-th particle can be represented by a *D*-dimensional vector $X_i = [x_{i1}, x_{i2}, \cdots, x_{iD}]^T$, which is also a potential solution to the problem, the speed of the *i*-th particle is V_i, the individual adjustment value is $P_i = [p_{i1}, p_{i2}, \cdots, p_{iD}]^T$, and the overall value of the population is $P_g = \left[p_{g1}, p_{g2}, \cdots, p_{gD}\right]^T$. The speed and position of the particle are updated in Eqs. 5 and 6, as follows:

$$V_{id}^{k+1} = \omega V_{id}^{k} + c_1 r_1 \left(P_{id}^{k} - X_{id}^{k}\right) + c_2 r_2 \left(P_{gd}^{k} - X_{gd}^{k}\right) \quad \text{(Eq. 5)}$$

$$X_{id}^{k+1} = X_{id}^{k} + V_{id}^{k+1} \quad \text{(Eq. 6)}$$

where, ω = inertia weights, $d, i \in [1, n]$, k = current iterations, V_{id} = speed of the particles under the current dimension, c_1 and c_2 = acceleration factors, and r_1 and r_2 = random number between the locations of $[0,1]$.

(4) Processing input and output samples

To better predict the difference between the predicted value and the true value, the mean absolute error (MAE), the root mean square error (RMSE), and the determination coefficient (R^2) were used as the evaluation criteria for the model, calculated using Eqs. 7, 8, and 9, respectively (Jha and Sit, 2021):

$$MAE = \frac{1}{n}\sum_{i=1}^{n}\left|Y_i - Y_i^*\right| \quad \text{(Eq. 7)}$$

$$RMSE = \sqrt{\frac{1}{n}\sum_{i=1}^{n}\left(Y_i - Y_i^*\right)^2} \quad \text{(Eq. 8)}$$

$$R^2 = \frac{\sum_{i=1}^{n}\left(Y_i^* - \bar{Y}_i\right)}{\sum_{i=1}^{n}\left(Y_i - \bar{Y}_i\right)} \quad \text{(Eq. 9)}$$

where, Y_i and Y_i^* = true and predicted values of the total flavonoid yields of purple potatoes during *I* training, respectively, and $\bar{Y}_i$ = average of the purple potato extract.

Determination of TFY

Using slightly modified method of Dewanto *et al*. (2002), rutin was used as the standard to analyse the total flavonoid content of purple potatoes. A stock solution of 0.2 mg/mL rutin was prepared and diluted to 0.02, 0.04, 0.06, 0.08, and 0.100 mg/mL concentrations for use as standard solutions. Next, 3 mL standard solution was added to the mixture, followed by the addition of 1.5 mL of 15% $NaNO_2$ solution, and stirred for 6 min. Next, 1.5 mL of 5% $Al(NO_3)_3$ solution was added to the solution, and stirred for 6 min. Then, 20 mL of 4% NaOH solution

was added, and stirred for 1 min. Finally, absorbance value A was measured at 510 nm to obtain a standard curve using the standard equation: $y = 0.4382x - 0.0027$, $R^2 = 0.9991$. Three millilitres of purple potato extract liquid in distilled water were used as a blank control.

Determination of antioxidant activity

Determination of OH· clearing capacity

The OH· clearance capacity was determined using a slightly modified methods of Wang *et al*. (2013). Briefly, the purple potato extract powder was dissolved in 70% ethanol, and diluted to the concentrations of 0.02, 0.03, 0.04, 0.05, 0.06, 0.12, and 0.24 mg/mL before analysis. A 0.5 mL sample of each concentration was mixed with 1 mL of 10 mmol/L salicylic acid-ethanol solution, 1 mL of 6 mL/L $FeSO_4$ solution, 1 mL of 6 mmol/L H_2O_2, and the oscillating mixture for 1 min. The mixture was incubated at 37°C in a water bath for 10 min, and absorbance was determined at 510 nm (A_1). Ethanol absorbance was also determined at 510 nm (A_0). Salicylic acid-ethanol solution and double-oxygen water absorbance was also determined at 510 nm (A_2). An equivalent concentration of vitamin C (Vc) was used as the positive control. The OH· clearance capacity was calculated using Eq. 10:

$$\text{OH·clearance}\frac{\text{rate}}{\%} = [1 - (A_1 - A_2)/A_0] \times 100\% \quad \text{(Eq. 10)}$$

Determination of DPPH· clearing capacity

The DPPH· clearance capacity was determined according to Hu *et al*. (2016) with slight adjustments. Briefly, the purple potato extract powder was dissolved in 70% ethanol, and diluted to 0.02, 0.03, 0.04, 0.05, 0.06, 0.12, and 0.24 mg/mL concentrations before analysis. Next, 0.5 mL sample of each concentration was mixed with 1.5 mL of 0.1 mmol/L DPPH in the dark for 0.5 h, and the absorbance value was measured at 517 nm; an equivalent concentration of Vc was used as the positive control. The DPPH· clearance capacity was calculated using Eq. 11:

$$\text{DPPH· clearance rate}/\% = (1 - A_1/A_0) \times 100\% \quad \text{(Eq. 11)}$$

where, A_1 and A_0 = absorbance values of the sample and DPPH· mixture, and ethanol and DPPH· mixture, respectively.

High-performance liquid chromatography (HPLC) analysis

The extract was subjected to HPLC analysis (Waters Inc., Milford, CT, USA) according to Xi *et al*. (2015), with minor modifications. Samples, rutin, quercetin, and kaempferol (5 mg each) were diluted in methanol to yield 0.2 mg/mL standard solutions. A total of 0.1 g of purple potato extract was dissolved in 25 mL of methanol. The extract was reconstituted to a test solution with a concentration of 4 mg/mL, and stored at 4°C until analysis. Test sample preparation: samples were filtered through a 0.45 μm membrane before the HPLC analysis, which was performed under following conditions: Zorbax Eclipse C18 chromatographic column, methanol-0.4% phosphoric acid (55:45) as the mobile phase, 1 mL/min flow rate, 30°C column temperature, 280 nm detection wavelength, and 10 μL of injection volume.

Fourier Transform Infrared Spectroscopy (FTIR) analysis

Samples were obtained under optimal conditions, frozen, and dried prior to the analysis. A scan was performed within the wavelength range of 400 - 4000 cm^{-1} using FTIR (Thermo Electron Inc., San Jose, CA, USA).

Statistical analysis

Each experiment was performed in three replicates. Data analysis and visualisation was performed using SPSS 26 ($p < 0.05$), Design Expert 13.0, Origin 2019, and MATLAB R2019a software.

Results and discussion

Effects of individual factors on TFY

Effects of enzyme addition on TFY

Figure 1A shows that the addition of enzymes at 30 - 50 U/mL concentrations substantially enhanced TFC extraction from purple potatoes. The TFY reached its peak of 7.82 mg/g when hemicellulose was added at 50 U/mL concentration. Elevated enzyme concentration enhances enzyme-substrate interaction kinetics. However, excessive enzyme addition reduced the TFY due to enzyme saturation, substrate inhibition, and increased solution viscosity, which created sub-optimal conditions for enzymatic activity and final product formation (Tchabo *et al*., 2015; Arbianti *et al*., 2023).

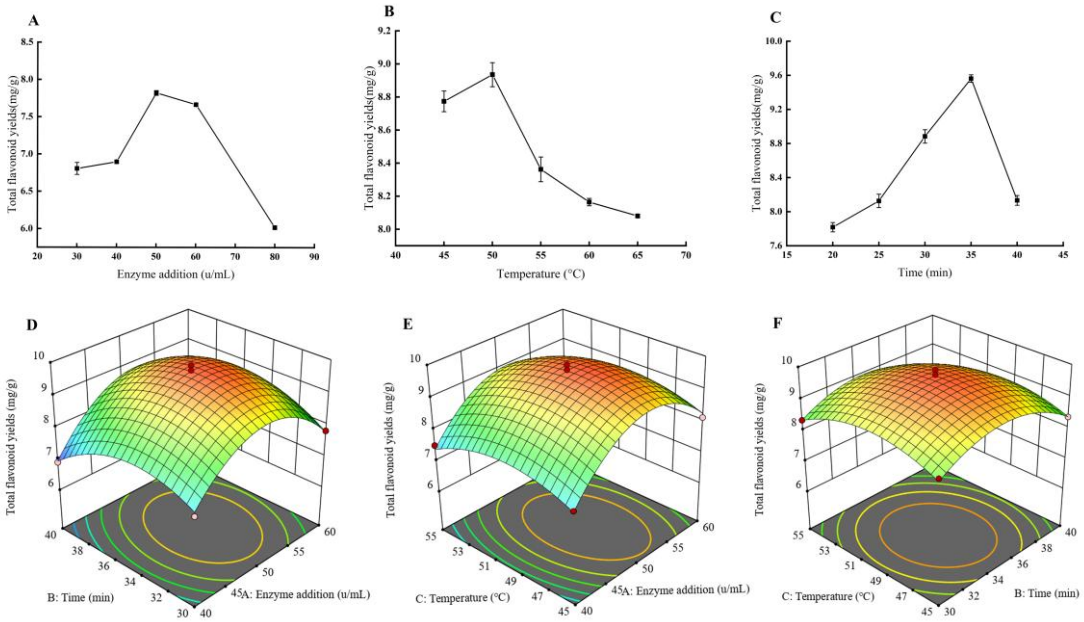

Figure 1. Effects of enzyme addition **(A)**, temperature **(B)**, and time **(C)** on total flavonoid yields; and response surface of interactive items' effects on total flavonoid yields [(**D**), (**E**), and (**F**)].

Effects of extraction temperature on TFY

As shown in Figure 1B, TFY decreased after an initial increase. Within 45–- 50°C, the TFY increased to a maximum of 8.93 mg/g at 50°C, but decreased as the temperature was increased further. An optimal ultrasonic temperature can facilitate the permeation of molecules, and enhance the solubility of flavonoid compounds, while temperatures higher than optimal, induce the degradation of soluble proteins, resulting in increased viscosity of the reaction system that prevents dissolution of flavonoid compounds. Certain flavonoids are degraded at high temperatures. Furthermore, the presence of dissolved contaminants in the solution can inhibit the extraction of total flavonoids (Xu *et al*., 2018; Liu *et al*., 2019).

Effects of extraction duration on TFY

Figure 1C shows that the TFY increased within 20 - 35 min, reaching a peak of 9.56 mg/g at 35 min, but decreased when the extraction time exceeded 35 min. An appropriate ultrasound extraction duration allowed the intracellular substances in purple potato cells to fully react with the enzymes and solvents, promoting the dissolution of flavonoid compounds. In contrast, longer ultrasound extraction duration promoted the dissolution of non-flavonoid substances, which may degrade the flavonoids, thus decreasing the TFY (Zhao *et al*., 2016; Liu *et al*., 2019).

RSM

The response factor and test level were determined based on the findings discussed earlier. The results of the response tests are listed in Table 1.

Differential and significance analyses for the regression model were performed using Design-Expert 13 software (Figure 2). Through multidimensional adjustment analysis, the corresponding regression equations for TFY, enzyme addition, extraction time, and extraction temperature were obtained as follows:

$$Y = 9.66 + 0.30 \times A - 0.12 \times B - 0.13 \times C + 0.21 \times AB - 0.04 \times AC - 0.04 \times BC - 1.32 \times A^2 - 0.77 \times B^2 - 0.57 \times C^2$$

The model summary statistics for TFY are shown in Table 2. Statistical significance was set at $p < 0.05$. Furthermore, to assess the suitability and sufficiency of the model, the coefficient of determination (R^2) and adjusted R^2 were calculated (Quanhong and Caili, 2005). The lack-of-fit analysis was conducted to determine whether the model explained the experimental data.

Our findings showed that the model findings were statistically significant ($p < 0.0001$), whereas the missing items were not significant, suggesting that the model was highly compatible. The coefficients of determination (R^2 = 0.9919) and adjustment

Table 1. Design and results of Box-Behnken experiment.

Number	Enzyme addition (U/mL)	Time (min)	Temperature (°C)	Total flavonoid yield (mg/g)
1	40	30	50	7.48
2	60	30	50	7.82
3	40	40	50	6.91
4	60	40	50	8.10
5	40	35	45	7.60
6	60	35	45	8.13
7	40	35	55	7.51
8	60	35	55	7.96
9	50	30	45	8.64
10	50	40	45	8.37
11	50	30	55	8.35
12	50	40	55	7.94
13	50	35	50	9.56
14	50	35	50	9.72
15	50	35	50	9.64
16	50	35	50	9.65
17	50	35	50	9.75

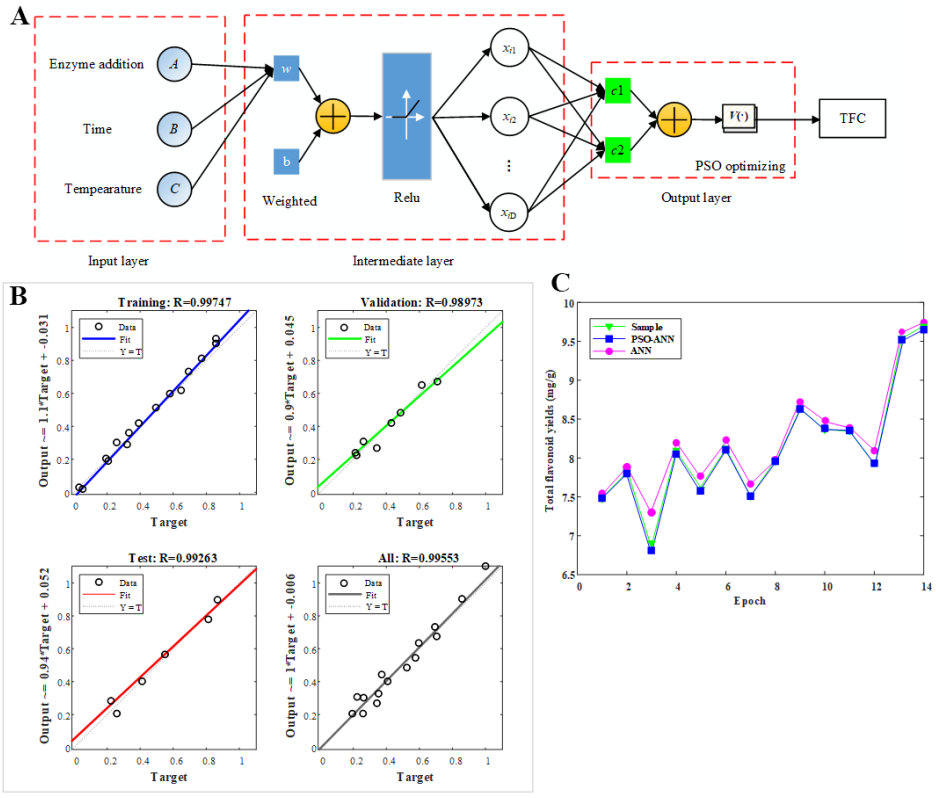

Figure 2. PSO-ANN model for ultrasonic wave extract of total flavonoid yields **(A)**; correlation coefficient *R*-value for training, validation, testing, and overall dataset **(B)**; and comparison effect diagram for total flavonoid yields of optimised ANN **(C)**.

Table 2. Results of analysis variance.

Source	Sum of squares	df	Mean square	*F*-value	*P*-value
Model	13.43	9	1.49	95.65	< 0.0001
A (enzyme addition)	0.73	1	0.74	46.50	0.0002
B (time)	0.12	1	0.12	7.66	0.0278
C (temperature)	0.14	1	0.14	9.19	0.0191
AB	0.18	1	0.18	11.56	0.0114
AC	8.0×10^{-3}	1	8.0×10^{-3}	0.51	0.4970
BC	5.2×10^{-3}	1	5.2×10^{-3}	0.34	0.5807
A^2	7.30	1	7.30	467.78	< 0.0001
B^2	2.48	1	2.48	158.83	< 0.0001
C^2	1.37	1	1.37	87.93	< 0.0001
Residual	0.11	7	0.016		
Lack of Fit	0.089	3	0.030	5.85	0.0605
Pure Error	0.020	4	5.1×10^{-3}		
Cor Total	13.54	16			
R^2	0.99				
Adj. R^2	0.98				

(R^2adj = 0.9816) values indicated that the model did not incorporate insignificant terms, and that its predictions closely matched the experimental values (Tchabo *et al*., 2015).

Among enzyme addition, extraction duration, and extraction temperature, A, B^2, and C^2 exhibited significance levels below 0.01, indicating a highly significant impact on TFY. In contrast, B, C, and AB demonstrated a significance level of < 0.05, indicating a substantial effect on TFY. The *F*-number indicated that the total flavonoids result was most influenced by A, followed by C and B.

Figures 1D - 1F show the peak-rising pattern for the response of each component interaction. The extraction rate of total flavonoids first increased and then decreased with the addition of enzymes, and increasing extraction temperature and extraction duration. The high-line diagram exhibited a closer resemblance to an ellipse, indicating a higher level of interaction. AB, AC, BC, and BC exhibited the strongest interactions, which corroborated the findings of differential analysis.

Based on Design Expert 9.0.6, an optimum extraction process for purple potato was analysed using a responsive test model with enzyme addition at 49.69 U/mL, extraction duration of 35.15 min, and extraction temperature of 49.77°C, with a theoretical extraction of TFY of 9.65 mg/g. When the process parameters were changed to 50 U/mL enzyme, extraction duration of 35 min, and an extraction temperature of 50°C, the TFY was 9.67 mg/g, and the actual relative error of the theoretical value was 1.78% ($p < 0.05$), indicating that RSM could be used to predict the conditions of total flavonoids extraction.

Results of PSO-ANN analysis

Next, experimental findings were subjected to ANN analysis using MATLAB R2019a software. Seventeen datasets were used as experimental samples for testing and validation, and PSO algorithm was used to optimise the parameters for optimum extraction conditions. The initial particle group size was set to 20, the learning rate and dynamic factor were both set to 0.01, the training number was set to 1000 times, and the adaptation function was a trained network model. These tests were performed to achieve a higher TFY. The developed neural network structure diagram contained three variables: the input and output neurons containing the TFY (Figure 2A).

In Figure 2B, the training-related coefficients of the PSO-ANN model are shown. When the iterations were 14 h, the training of the PSO-ANN neural network ended with an average error of 0.0053558, and the *R* values of the training, validation, and test data were 0.9977, 0.98973, and 0.99263, respectively, with a total *R* value of 0.99553. The values were close to 1, indicating that the

optimised neural-network model could be reliably used to analyse and optimise the conditions of the experimental process.

Figure 2C shows the pre- and post-training sets and sample values for the optimised artificial neural networks. Based on optimised analysis, 51.34 U/mL, 36.21 min, and 53.12°C were the ideal extraction process parameters for enzyme amount, extraction duration, and extraction temperature, respectively, with the theoretical TFY being 9.81 mg/g. Similarly, the modified process conditions were adjusted to an enzyme addition of 51 U/mL, an extraction duration of 36 min, and an extraction temperature of 53°C. Under these conditions, the TFY was 9.82 mg/g, and the relative error of the test value to the theoretical value was 0.10%, which was not significant, and the test result was higher than the RSM value. Previous studies on the optimisation of bioactive compound extraction processes have demonstrated that both RSM and ANN models exhibited robust predictive capabilities, with ANN often outperforming RSM in terms of non-linear parameter interactions and generalisation accuracy (Said *et al*., 2020; Onukwuli *et al*., 2021; Wu *et al*., 2024).

Validation trial results

A comparison of the extraction processes after the optimisation of the two models is shown in Table 3. The predicted values in both the RSM and PSO-ANN methods were close to the real values under optimal conditions, and the relative error value of PSO-ANN was significantly lower than that of the RSM method, and was closer to the actual extraction results. These findings suggested that the method could provide a reference for optimising the process of extracting total flavonoids.

Table 3. Comparison between predicted and experimental values for optimal conditions of RSM and PSO-ANN.

Optimisation method	Enzyme addition (U/mL)	Time (min)	Temperature (°C)	Total flavonoid yield (mg/g)		RE (%)
				Predicted value	Experimental value	
RSM	50	35	50	9.65	9.67	0.21
PSO-ANN	51	36	53	9.81	9.82	0.10

Analysis of antioxidant activity

Figure 3A shows a rapid increase in OH·clearance rate from 33.9 to 76.8% when the concentration of the purple potato extract increased from 0.02 to 0.12 mg/mL. As the purple potato extract concentration increased, the OH· clearance rate gradually increased, reaching a maximum of 81.6%. At equivalent concentrations, Vc exhibited a superior ability to eliminate OH· compared to purple potato extract. The IC_{50} value of the purple potato extract (0.037 mg/mL) was slightly higher than that of Vc (0.013 mg/mL), indicating its strong radical scavenging activity.

Figure 3B shows that as the concentration of purple potato extract increased from 0.02 to 0.06 mg/mL, the rate at which DPPH· was cleared increased significantly from 11.6 to 40.1%. As the purple potato extract concentration increased further, the rate of DPPH· clearance gradually reached 61.8%. At equivalent concentrations, The IC_{50} value of the purple potato extract (0.12 mg/mL) was slightly higher than that of Vc (0.029 mg/mL), indicating its ability to scavenge DPPH radicals and its potential antioxidant efficacy.

HPLC analysis

HPLC is widely employed for the identification and quantification of flavonoids due to its exceptional precision, sensitivity, and reproducibility in analysing complex matrices (Blunder *et al*., 2017; Mizzi *et al*., 2020; Teuta *et al*., 2024). The analysis of the purple potato extracts is shown in Figures 3C and 3D. Figure 3C shows a chromatogram illustrating retention times of standard chemicals rutin, quercetin, and kaempferol as 5.1137, 11.3913, and 19.1250 min, respectively. Figure 3D shows the chromatogram of the purple potato extract. We observed three distinct peaks with retention times of 5.1157, 11.4317, and 19.2150 min, respectively. These retention times corresponded to those of rutin, quercetin, and kaempferol. Additional chemicals showing peaks were not identified; therefore, further research is necessary to identify them.

FTIR analysis

FTIR has emerged as a prominent analytical tool for food chemistry and offers rapid, precise, and cost-effective results that require minimal sample volumes. Its high sensitivity and ability to preserve

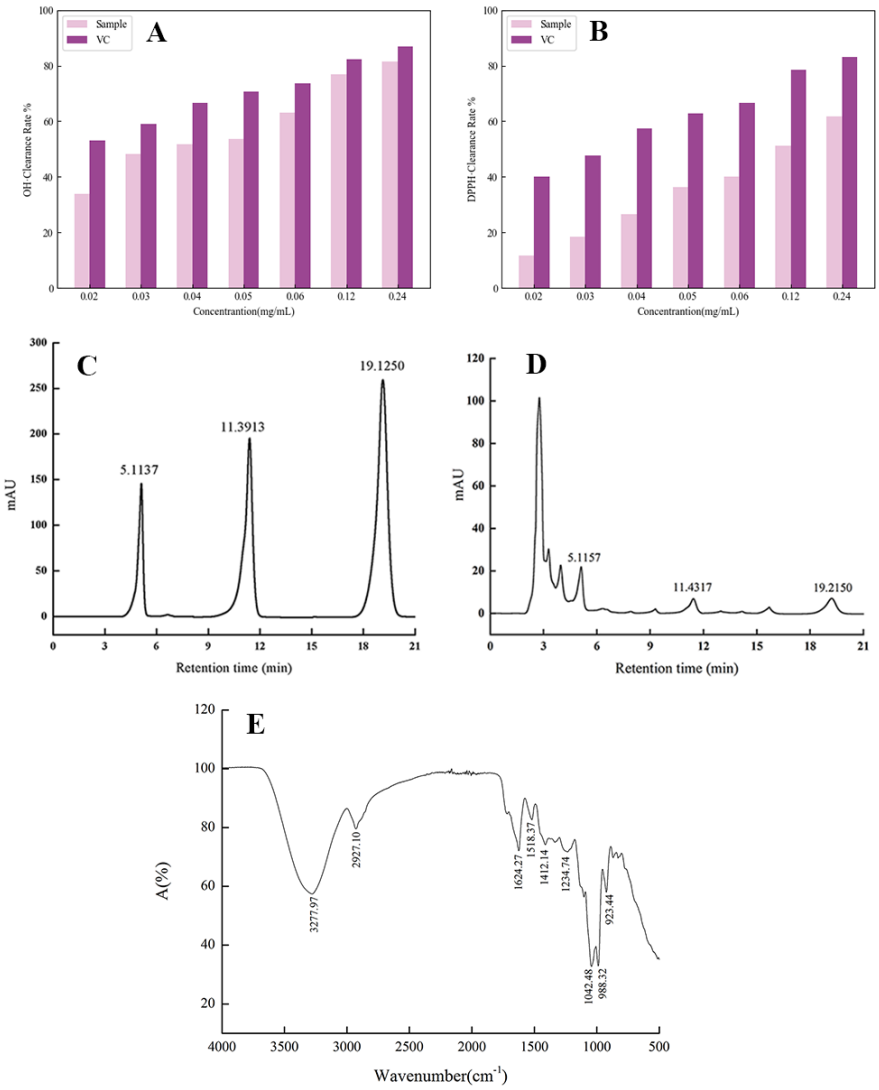

Figure 3. Scavenging effect on OH· and DPPH· [**(A)** and **(B)**], HPLC chromatogram [**(C)** and **(D)**], and infrared spectrogram of sample **(E)**.

compound structures further enhance its applicability in complex matrix analyses (Lu *et al*., 2011; Zheng *et al*., 2017; Baltacıoğlu *et al*., 2024). Figure 3E shows the FTIR spectral features of the purple potato extract. The absorption peak at 3277.97 cm^{-1} can be attributed to the presence of -OH, while the weaker absorption peak at 2927.10 cm^{-1} can be attributed to the presence of a C-H bond (Thummajitsakul *et al*., 2020). The stronger peak at 1624.27 cm^{-1} can be attributed to the C=O bond (Lu *et al*., 2011), whereas the weaker peak at 1518.37 cm^{-1} can be attributed to the in-plane C-H bending vibration of the aromatic phenyl rings (Schulz and Baranska, 2007). Furthermore, alkyl stretching vibration was responsible for the absorption peak at 1042.48 cm^{-1}, the C=C bond of cyclobenzene can be attributed to the peak at 988.32 and 923.44 cm^{-1} (Baltacıoğlu *et al*., 2024). The FTIR spectral features displayed characteristic absorption peaks corresponding to flavonoid functional groups, indicating the presence of flavonoid compounds in the extracts (Colombo *et al*., 2019). The consistency between the HPLC quantification and FTIR spectral data validated the efficacy of the UAEE method.

Conclusion

The present work demonstrated the optimum conditions for the extraction of total flavonoids using RSM and PSO-ANN methods. Both the models exhibited superior reliability than that of traditional methods. Furthermore, the PSO-ANN model predicted relatively small errors in total flavonoid extraction with higher determination factors, and the best conditions for the extraction process. The purple potato extract contained flavonoids as confirmed by performing ultraspectral and HPLC analyses. The

elimination of OH· and DPPH· demonstrated the presence of antioxidant activity of the purple potato extracts. In summary, the PSO-ANN model demonstrated high efficiency in optimising and predicting the extraction processes. This innovative approach for extracting bioactive compounds from purple potatoes established a robust framework with significant implications for the food and pharmaceutical industries. This approach will enable the development of antioxidant-rich functional foods and support the scalable, sustainable extraction of bioactive compounds from diverse dietary sources.

Acknowledgement

The present work was financially supported by the Natural Science Project, Bengbu Medical University (grant no.: 2021byzd026) and Key Scientific Research Project of Anhui Provincial Department of Education (grant nos.: 2024AH051218, 2024AH051244). The authors acknowledge the Experimental Centre for Food and Pharmaceutical Engineering, Bengbu Medical University for the research facilities.

References

Ahmad-Qasem, M. H., Cánovas, J., Barrajón-Catalán, E., Micol, V., Cárcel, J. A. and García-Pérez, J. V. 2013. Kinetic and compositional study of phenolic extraction from olive leaves (var. Serrana) by using power ultrasound. Innovative Food Science and Emerging Technologies 17: 120-129.

Amiri-Rigi, A., Abbasi, S. and Scanlon, M. G. 2016. Enhanced lycopene extraction from tomato industrial waste using microemulsion technique: Optimisation of enzymatic and ultrasound pre-treatments. Innovative Food Science and Emerging Technologies 35: 160-167.

Arbianti, R., Suryapranata, B., Latifah, L. P., Putri, N. F., Utami, T. S. and Muharam, Y. 2023. Combined enzymatic and ultrasound-assisted aqueous two-phase extraction of antidiabetic flavonoid compounds from *Strobilanthes crispus* leaves. Communications in Science and Technology 8(2): 113-123.

Badshah, S. L., Faisal, S., Muhammad, A., Poulson, B. G., Emwas, A. H. and Jaremko, M. 2021. Antiviral activities of flavonoids. Biomedicine and Pharmacotherapy 140: 111596.

Baltacıoğlu, C., Baltacıoğlu, H., Okur, İ., Yetişen, M. and Alpas, H. 2024. Recovery of phenolic compounds from peach pomace using conventional solvent extraction and different emerging techniques. Journal of Food Science 89(3): 1672-1683.

Blunder, M., Orthaber, A., Bauer, R., Bucar, F. and Kunert, O. 2017. Efficient identification of flavones, flavanones and their glycosides in routine analysis *via* off-line combination of sensitive NMR and HPLC experiments. Food Chemistry 218: 600-609.

Cai, Z., Qu, Z., Lan, Y., Zhao, S., Ma, X., Wan, Q., ... and Li, P. 2016. Conventional, ultrasound-assisted, and accelerated-solvent extractions of anthocyanins from purple sweet potatoes. Food Chemistry 197: 266-272.

Chen, X., Jia, X., Yang, S., Zhang, G., Li, A., Du, P., ... and Li, C. 2022. Optimization of ultrasonic-assisted extraction of flavonoids, polysaccharides, and eleutherosides from *Acanthopanax senticosus* using response surface methodology in development of health wine. LWT - Food Science and Technology 165: 113725.

Ciric, A., Krajnc, B., Heath, D. and Ogrinc, N. 2020. Response surface methodology and artificial neural network approach for the optimization of ultrasound-assisted extraction of polyphenols from garlic. Food and Chemical Toxicology 135: 110976.

Colombo, M., de Lima Melchiades, G., Michels, L. R., Figueiró, F., Bassani, V. L., Teixeira, H. F. and Koester, L. S. 2019. Solid dispersion of kaempferol: Formulation development, characterization, and oral bioavailability assessment. AAPS PharmSciTech 20: 1-9.

Corcoran, M. P., McKay, D. L. and Blumberg, J. B. 2012. Flavonoid basics: Chemistry, sources, mechanisms of action, and safety. Journal of Nutrition in Gerontology and Geriatrics 31(3): 176-189.

Dewanto, V., Wu, X., Adom, K. K. and Liu, R. H. 2002. Thermal processing enhances the nutritional value of tomatoes by increasing total antioxidant activity. Journal of Agricultural and Food Chemistry 50(10): 3010-3014.

Esatbeyoglu, T., Rodríguez-Werner, M., Schlösser, A., Winterhalter, P. and Rimbach, G. 2017. Fractionation, enzyme inhibitory and cellular antioxidant activity of bioactives from purple sweet potato (*Ipomoea batatas*). Food Chemistry 221: 447-456.

Hornik, K., Stinchcombe, M. and White, H. 1989. Multilayer feedforward networks are universal approximators. Neural Networks 2(5): 359-366.

Hou, M. Y., Hu, W. Z., Wang, A. S., Xiu, Z. L., Shi, Y. S., Hao, K. X., ... and Sun, J. 2019. Ultrasound-assisted extraction of total flavonoids from *Pteris cretica* L.: Process optimization, HPLC analysis, and evaluation of antioxidant activity. Antioxidants 8(10): 425.

Hu, Y. J., Deng, L., Chen, J., Zhou, S., Liu, S., Fu, Y., ... and Chen, M. 2016. An analytical pipeline to compare and characterise the anthocyanin antioxidant activities of purple sweet potato cultivars. Food Chemistry 194: 46-54.

Huang, H., Xu, Q., Belwal, T., Li, L., Aalim, H., Wu, Q., ... and Luo, Z. 2019. Ultrasonic impact on viscosity and extraction efficiency of polyethylene glycol: A greener approach for anthocyanins recovery from purple sweet potato. Food Chemistry 283: 59-67.

Jha, A. K. and Sit, N. 2021. Comparison of response surface methodology (RSM) and artificial neural network (ANN) modelling for supercritical fluid extraction of phytochemicals from *Terminalia chebula* pulp and optimization using RSM coupled with desirability function (DF) and genetic algorithm (GA) and ANN with GA. Industrial Crops and Products 170: 113769.

Liu, J., Mu, T., Sun, H. and Fauconnier, M. L. 2019. Optimization of ultrasonic-microwave synergistic extraction of flavonoids from sweet potato leaves by response surface methodology. Journal of Food Processing and Preservation 43(5): e13928.

Liu, Y., Chen, F. and Guo, H. 2017. Optimization of bayberry juice spray drying process using response surface methodology. Food Science and Biotechnology 26: 1235-1244.

Lu, X., Wang, J., Al-Qadiri, H. M., Ross, C. F., Powers, J. R., Tang, J. and Rasco, B. A. 2011. Determination of total phenolic content and antioxidant capacity of onion (*Allium cepa*) and shallot (*Allium oschaninii*) using infrared spectroscopy. Food Chemistry 129(2): 637-644.

Luo, D., Mu, T. and Sun, H. 2021. Profiling of phenolic acids and flavonoids in sweet potato (*Ipomoea batatas* L.) leaves and evaluation of their anti-oxidant and hypoglycemic activities. Food Bioscience 39: 100801.

Mizzi, L., Chatzitzika, C., Gatt, R. and Valdramidis, V. 2020. HPLC analysis of phenolic compounds and flavonoids with overlapping peaks. Food Technology and Biotechnology 58(1): 12-19.

Nag, S. and Sit, N. 2018. Optimization of ultrasound assisted enzymatic extraction of polyphenols from pomegranate peels based on phytochemical content and antioxidant property. Journal of Food Measurement and Characterization 12: 1734-1743.

Onukwuli, D. O., Esonye, C., Ofoefule, A. U. and Eyisi, R. 2021. Comparative analysis of the application of artificial neural network-genetic algorithm and response surface methods-desirability function for predicting the optimal conditions for biodiesel synthesis from *Chrysophyllum albidum* seed oil. Journal of the Taiwan Institute of Chemical Engineers 125: 153-167.

Panche, A. N., Diwan, A. D. and Chandra, S. R. 2016. Flavonoids: An overview. Journal of Nutritional Science 5: e47.

Quanhong, L. and Caili, F. 2005. Application of response surface methodology for extraction optimization of germinant pumpkin seeds protein. Food Chemistry 92(4): 701-706.

Riciputi, Y., Diaz-de-Cerio, E., Akyol, H., Capanoglu, E., Cerretani, L., Caboni, M. F. and Verardo, V. 2018. Establishment of ultrasound-assisted extraction of phenolic compounds from industrial potato by-products using response surface methodology. Food Chemistry 269: 258-263.

Said, F. M., Gan, J. Y. and Sulaiman, J. 2020. Correlation between response surface methodology and artificial neural network in the prediction of bioactive compounds of unripe *Musa acuminata* peel. Engineering Science and Technology 23(4): 781-787.

Samsonowicz, M., Regulska, E., Karpowicz, D. and Leśniewska, B. 2019. Antioxidant properties of coffee substitutes rich in polyphenols and minerals. Food Chemistry 278: 101-109.

Schulz, H. and Baranska, M. 2007. Identification and quantification of valuable plant substances by IR and Raman spectroscopy. Vibrational Spectroscopy 43(1): 13-25.

Singla, M. and Sit, N. 2021. Application of ultrasound in combination with other technologies in food processing: A review. Ultrasonics Sonochemistry 73: 105506.

Steed, L. E. and Truong, V. D. 2008. Anthocyanin content, antioxidant activity, and selected physical properties of flowable purple-fleshed sweet potato purees. Journal of Food Science 73(5): S215-S221.

Tchabo, W., Ma, Y., Engmann, F. N. and Zhang, H. 2015. Ultrasound-assisted enzymatic extraction (UAEE) of phytochemical compounds from mulberry (*Morus nigra*) must and optimization study using response surface methodology. Industrial Crops and Products 63: 214-225.

Teuta, J. P., Narváez-Cuenca, C. E. and Murillo, M. Á. 2024. A high-performance liquid chromatography method validation and a Box-Behnken experimental design for the extraction optimization of quercitrin from *Nectandra reticulata*. RSC Advances 14(30): 21874-21886.

Thummajitsakul, S., Samaikam, S., Tacha, S. and Silprasit, K. 2020. Study on FTIR spectroscopy, total phenolic content, antioxidant activity and anti-amylase activity of extracts and different tea forms of *Garcinia schomburgkiana* leaves. LWT - Food Science and Technology 134: 110005.

Wang, F., Zhang, S., Deng, G., Xu, K., Xu, H. and Liu, J. 2022. Extracting total anthocyanin from purple sweet potato using an effective ultrasound-assisted compound enzymatic extraction technology. Molecules 27(14): 4344.

Wang, S., Dong, X. and Tong, J. 2013. Optimization of enzyme-assisted extraction of polysaccharides from alfalfa and its antioxidant activity. International Journal of Biological Macromolecules 62: 387-396.

Wu, H., Zhu, J., Diao, W. and Wang, C. 2014. Ultrasound-assisted enzymatic extraction and antioxidant activity of polysaccharides from pumpkin (*Cucurbita moschata*). Carbohydrate Polymers 113: 314-324.

Wu, J., Yang, F., Guo, L. and Sheng, Z. 2024. Modeling and optimization of ellagic acid from Chebulae Fructus using response surface methodology coupled with artificial neural network. Molecules 29(16): 3953.

Xi, L., Mu, T. and Sun, H. 2015. Preparative purification of polyphenols from sweet potato (*Ipomoea batatas* L.) leaves by AB-8 macroporous resins. Food Chemistry 172: 166-174.

Xu, L., He, W., Lu, M., Yuan, B., Zeng, M., Tao, G., ... and He, Z. 2018. Enzyme-assisted ultrasonic-microwave synergistic extraction and UPLC-QTOF-MS analysis of flavonoids from Chinese water chestnut peels. Industrial Crops and Products 117: 179-186.

Zhao, Y. M., Wang, J., Wu, Z. G., Yang, J. M., Li, W. and Shen, L. X. 2016. Extraction, purification and anti-proliferative activities of polysaccharides from *Lentinus edodes*. International Journal of Biological Macromolecules 93: 136-144.

Zheng, X., Hu, Y., Anggreani, E. and Lu. X. 2017. Determination of total phenolic content and antioxidant capacity of blueberries using Fourier transformed infrared (FT-IR) spectroscopy and Raman spectroscopy. Journal of Food Measurement and Characterization 11: 1909-1918.